

# Effects of different doses of cadmium on secondary metabolites and gene expression in *Artemisia annua* L.

Liangyun Zhou<sup>1,\*</sup>, Guang Yang<sup>1,\*</sup>, Haifeng Sun<sup>2</sup>, Jinfu Tang<sup>1</sup>, Jian Yang<sup>1</sup>, Yizhan Wang<sup>3</sup>, Thomas Avery Garran<sup>1</sup>, Lanping Guo (✉)<sup>1</sup>

<sup>1</sup>The State Key Laboratory Breeding Base of Dao-di Herbs, National Resource Center for Chinese Materia Medica, China Academy of Chinese Medical Sciences, Beijing 100700, China; <sup>2</sup>College of Chemistry and Chemical Engineering, Shanxi University, Taiyuan 030006, China; <sup>3</sup>Eye Hospital, China Academy of Chinese Medical Sciences, Beijing 100523, China

© Higher Education Press and Springer-Verlag Berlin Heidelberg 2016

**Abstract** This study aims to elucidate the underlying molecular mechanisms of artemisinin accumulation induced by cadmium (Cd). The effects of different Cd concentrations (0, 20, 60, and 120  $\mu\text{mol/L}$ ) on the biosynthesis of *Artemisia annua* L. were examined. Intermediate and end products were quantified by HPLC-ESI-MS/MS analysis. The expression of key biosynthesis enzymes was also determined by qRT-PCR. The results showed that the application of treatment with 60 and 120  $\mu\text{mol/L}$  Cd for 3 days significantly improved the biosynthesis of artemisinic acid, arteannuin B, and artemisinin. The concentrations of artemisinic acid, arteannuin B, and artemisinin in the 120  $\mu\text{mol/L}$  Cd-treated group were 2.26, 102.08, and 33.63 times higher than those in the control group, respectively. The concentrations of arteannuin B and artemisinin in 60  $\mu\text{mol/L}$  Cd-treated leaves were 61.10 and 26.40 times higher than those in the control group, respectively. The relative expression levels of *HMGR*, *FPS*, *ADS*, *CYP71AV1*, *DBR2*, *ALDH1*, and *DXR* were up-regulated in the 120  $\mu\text{mol/L}$  Cd-treated group because of increased contents of artemisinic metabolites after 3 days of treatment. Hence, appropriate doses of Cd can increase the concentrations of artemisinic metabolites at a certain time point by up-regulating the relative expression levels of key enzyme genes involved in artemisinin biosynthesis.

**Keywords** Cd; secondary metabolites; gene expressions; *Artemisia annua* L.

## Introduction

Secondary metabolites in plants are the products of long-term evolution in a particular environment; these compounds play important roles in many vital activities [1,2]. The development of an ecotype within a habitat could significantly affect the accumulation of secondary metabolites. Heavy metal pollution in soil and environmental stresses such as drought, pest, and disease damage, are vital factors that affect secondary metabolite accumulation. Pollution of cadmium (Cd), one of the most poisonous heavy metals, causes physiological and biochemical damages to plants; these damages include inhibited seed germination and plant growth [3,4],

decreased photosynthetic efficiency [5,6], and varied uptake rates of soil ions [7]. In addition, Cd can alter the biosynthesis of secondary metabolites and their related gene expression. Vitti *et al.* showed that the amount of IAA in *Arabidopsis thaliana* roots treated with Cd was significantly higher than that in the control group; the expression of *AtIPT* in the shoot and *AtCKX* in the root was significantly up-regulated after Cd treatment [8]. Daud *et al.* showed that the malondialdehyde (MDA) concentrations in the leaves, stems, and roots of two transgenic cotton cultivars treated with 1000  $\mu\text{mol/L}$  Cd were higher than those in their respective controls, except in the roots of BR001; the highest MDA concentrations were found in the roots of GK30 [9]. Thus far, the effects of Cd on medicinal plants, particularly on the biosynthesis of active substances, have been rarely investigated [10,11].

The above-ground parts of *Artemisia annua*, a therophyte from the Asteraceae family, is a traditional Chinese medicine, known as *qinghao*, used to clear vacuity heat,

Received April 1, 2016; accepted August 26, 2016

Correspondence: glp01@126.com

\*Liangyun Zhou and Guang Yang contributed equally to this study.

cool the blood, and prevent malaria. Modern pharmacological research shows that artemisinin (AN) is the main ingredient for malaria prevention. In 2001, the World Health Organization recommended artemisinin combination therapies (ACT) as the first-line therapy for malaria worldwide. Since its discovery, commercial preparations of artemisinin have been mainly isolated from plants. Studies show that wounding [12], water [13], chitosan [14], sugars [15], salicylic acid [16], and MeJA [17] enhanced the biosynthesis of artemisinin metabolites by upregulating the expression of key enzyme genes in the biosynthesis pathways. However, gene expression and increased rate differ when different elicitors are used. For example, MeJA upregulated *CYP71AV1*, and miconazole enhanced *CPR* and *DBR2* expression [17].

AN is mainly produced and stored in the glandular secretory trichomes on leaves, stems, and inflorescences [18] of *A. annua*. Fig.1 shows the possible pathways of AN biosynthesis. In the plant, AN is biosynthesized from farnesyl pyrophosphate (FPP) produced from isopentenyl pyrophosphate (IPP), which is derived from the mevalonate (MVA) and the 2C-methyl-D-erythritol4-phosphate (MEP) pathway [16,19,20]. FPP is converted into amorpho-4,11-diene cyclized by amorpho-4,11-diene synthase (ADS) [21]. Amorpho-4,11-diene is then converted into artemisinic acid (AA). In this step, cytochrome P450 monooxygenase (*CYP71AV1*) hydroxylate amorpho-4,11-dieneto produces artemisinic alcohol, which oxidizes to generate AA via artemisinic aldehyde [22,23]. The final step is the generation of dihydroartemisinic acid (DHAA) formed from artemisinic aldehyde through dihydroartemisinic aldehyde. Scholars reported that the final step involves two genes, namely, a double bond reductase (*DBR2*) [24] and an aldehyde dehydrogenase (*ALDH1*) [25]. Furthermore, DHAA scavenges reactive oxygen species (ROS) and is converted into AN through a non-enzymatic spontaneous reaction [26,27]. In addition, arteannuin B (AB), which is generated from artemisinic acid (AA), may be converted into AN [14].

Our previous work showed that Cd enhanced the accumulation of artemisinin and its precursors in *A. annua*; however, the underlying mechanism remains unclear [10,28]. Our team aims to understand the effects of Cd on the accumulation of secondary metabolites in *A. annua* and provide a basis for further studies on other pharmacologically active medicinal plants. In the present study, the effects and the mechanisms of Cd on the accumulation of other secondary metabolites such as AA, AB, and DHAA, were investigated using different Cd concentrations. *A. annua* was grown in a controlled hydroponic environment and treated with different concentrations of Cd. Leaves were collected at different time periods after the treatment. Four secondary metabolites and eight key enzyme genes involved in AN synthesis were analyzed.

## Materials and methods

### Plant material and experimental design

*A. annua* seeds (guihao third) were obtained from the National Engineering Laboratory of South-west Endangered Medicinal Resources Development. The seeds were sown with 2/3 sterilized vermiculite and watered with distilled water and Hoagland solution every day. Thereafter, the plants were watered every 3 days. When seedlings reached a height of 5 cm, they were transferred to hydroponic pots with 1 L of Hoagland solution (pH 5.8). Three seedlings of the same height were transplanted into each pot. The Hoagland solution was changed every 2 days.

Plants were grown in a greenhouse with a 12 h/12 h (light/dark) photo-period with sodium lighting at 25 °C. The seedlings were grown for 40 days. Four different Cd ( $\text{Cd}(\text{NO}_3)_2 \cdot 4\text{H}_2\text{O}$ ) concentrations was added to the Hoagland solution: 0 (control group), 20, 60, and 120  $\mu\text{mol/L}$ . Each Cd level was replicated nine times, with each group consisting of three pots containing nine seedlings.

### Solution preparation

Briefly, 20.0 mg of the AN standard was weighed and dissolved in 10 ml of methyl alcohol to obtain a standard stock solution (2000  $\mu\text{g/ml}$ ). The stock solution was diluted to 500.0, 200.0, 100.0, 50.0, 20.0, 10.0, and 5.0  $\mu\text{g/ml}$  by adding methyl alcohol and stored at 4 °C. Moreover, 2 mg of AA, AB, and DHAA standards were weighed and dissolved in 10 ml of methyl alcohol to obtain stock solutions of 200  $\mu\text{g/ml}$ . The solutions were diluted to 50.0, 20.0, 10.0, 5.0, 2.0, 2.0, and 0.5  $\mu\text{g/ml}$  with methyl alcohol and stored at 4 °C.

One plant from each hydroponic pot was harvested at 0, 1, and 3 days (d) after Cd treatment and dried to a constant weight in a ventilated oven at 45 °C. *A. annua* was extracted according to previously reported method with slight modifications [29]. Dry crushed plant material (0.20 g) was weighed in an Eppendorf tube. The samples were sonicated in 2.5 ml of methanol for 20 min at 30 °C and centrifuged at 12 000 r/min for 5 min. The supernatant was transferred to a 10-ml volumetric flask. The procedure was repeated twice, and respective supernatants were combined. The final volume was adjusted to volume with methanol and mixed thoroughly. After filtration with 0.22  $\mu\text{m}$  nylon membrane filter (Agela Technologies, Tianjin, China), the extract was used to quantify AA, AB, DHAA, and AN in *A. annua*.

### HPLC-ESI-MS/MS analysis

Chromatographic analyses were performed on an Agilent 1220 Infinity System (Agilent Corporation, CA, USA).

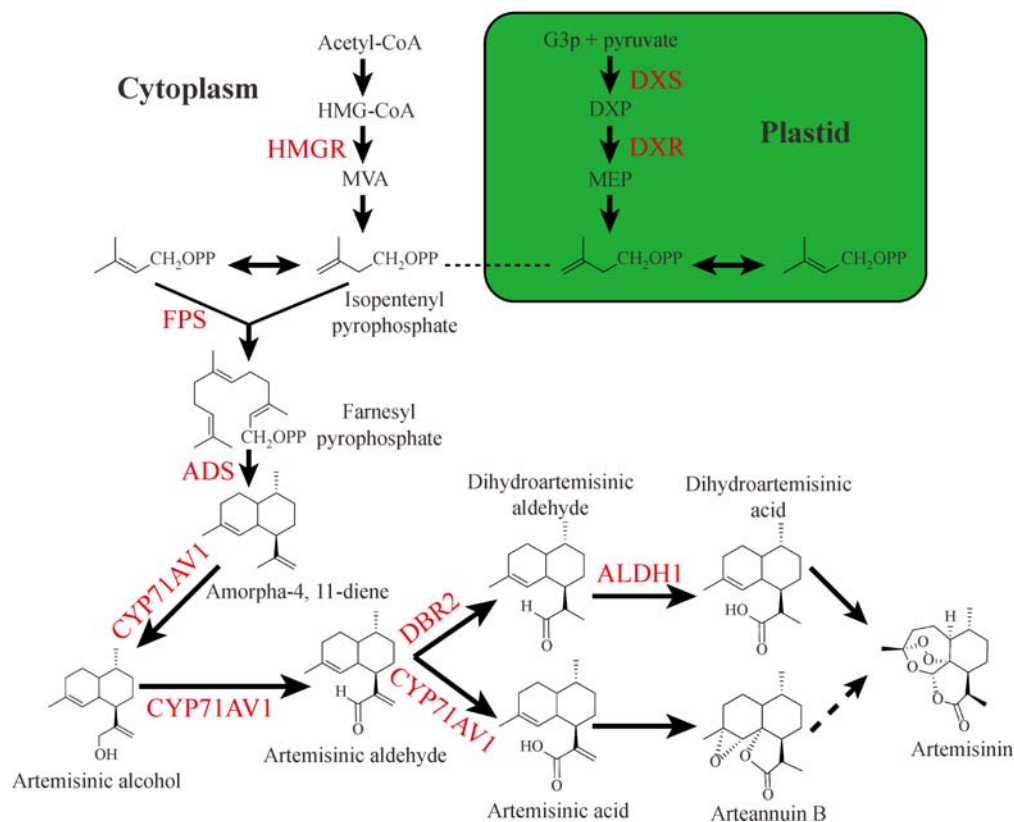


**Fig. 1** Possible pathways of artemisinin biosynthesis in *A. annua* (AA, artemisinic acid; AB, arteannuin B; DHAA, dihydroartemisinic acid; and AN, artemisinin).

HPLC separation was carried out on ZORBAX RRHD Eclipse Plus C<sub>18</sub> column (2.1 mm × 50 mm, 1.8 μm, Agilent Technologies, MD, USA) with the thermostat set at 30 °C. The injection volume for all samples was 5 μl, and the flow rate was 0.200 ml/min. The binary gradient consisted of solvent system A (formic acid/acetonitrile 0.1:99.9 v/v) and solvent system B (formic acid/water 0.1:99.9 v/v). The conditions were as follows: 0 min, 25% A; 7 min, 98% A; 9.5 min, 98% A; 10 min, 25% A; 15 min, 25% A; and isocratic at 25% A from 15 to 20 min to create equilibrium in the column for the next injection. For ESI-MS/MS analysis, an Agilent QQQ 6420 Mass Spectrometer (Santa Clara, CA, USA) was connected on the same Agilent 1220 HPLC instrument via an electrospray ionization (ESI) interface. MS analysis was carried out in positive ionization mode (ESI<sup>+</sup>) by monitoring the protonated molecular ions under the following operating conditions: nebulizer gas pressure of 30.00 psi; dry gas flow rate of 10.00 L/min; ion source electrospray voltage of 4000 V; and capillary temperature of 350 °C. The MS parameters were manually optimized (Table 1). Quantification was performed using multiple reaction monitoring (MRM) modes for the above transitions. Data were acquired with Agilent MassHunter Workstation

Acquisition software and analyzed using Agilent MassHunter Workstation Qual software.

#### Extraction of total RNA and real-time PCR analysis

Leaves were collected from *A. annua* at 0, 4, 8, 12, 24, 48, and 72 h after the treatment, immediately frozen in liquid nitrogen, and stored at −80 °C until further use. Total RNA was extracted from the samples using RNeasy Plant Mini Kit. DNase treatment was performed on an RNeasy Mini spin column with RNase-free DNase set (QIAGEN, Germany) according to the manufacturer's protocol. Approximately 0.5 μg of total RNA was reverse transcribed using Primer Script™ II 1st Strand cDNA Synthesis Kit (Takara, Japan) according to the manufacturer's instructions.

Real-time PCR (qPCR) was performed using specific primers designed by the online PrimerQuest Tool (Table 2) on 7500 qPCR equipment (Applied Biosystems, USA). First-strand cDNA was used as template in 10-μl reactions including 5 μl of Power SYBR Green PCR Master Mix (Applied Biosystems, USA) and 0.025 μg of each primer. qPCR cycling was performed at 50 °C (2 min), 95 °C (10 min), 40 cycles at 95 °C (15 s), 60 °C (1 min), and finally a

**Table 1** Analysis of MS parameters of the four compounds

Analytes	MRM transitions ( <i>m/z</i> )	Fragmentor (V)	Collision energy (eV)
AA	235 → 200	150	10
AB	249 → 189	100	5
DHAA	237 → 200	150	10
AN	283 → 247	100	5

**Table 2** Nucleotide sequences of primers used in real-time PCR

Gene ID	Forward primer sequence (5' to 3') / reverse primer sequence (5' to 3')	Product size (bp)
<i>Actin</i> (EU531837)	CCAGGCTGTTTCAGTCTCTGTAT CGCTCGGTAAGGATCTTCATCA	180
<i>HMGR</i> (AF142473)	GTAAGCTGCCACCCAAACCA AGTAAGCGACTGAGAAGAATAAGG	159
<i>FPS</i> (GQ420346)	ATACCTGGAGGAAAGCTGAACC CAACCAAGGGCAGATGAAAG	110
<i>ADS</i> (JQ319661)	CGAATGGGCTGTCTCTGC CTTCATATAACTTTCAAGGCTCG	133
<i>CYP71A1</i> (DQ453967)	CGAGACTTTAACTGGTGAGATTGT CGAAGCGACTGAAATGACTTTACT	144
<i>ALDH1</i> (FJ809784)	ATGGACTTGCCTCAGGTGTAT TGCCTCTAATCCTTGTCTCG	170
<i>DBR2</i> (EU704257)	GCGGTGGTTACTACTAGAGAAGT ATAATCAAACTAGAGGAGTGACCC	228
<i>DXS</i> (AF182286)	GTGCTTCCAGACCGTTACATTGA AGCCTCTCGTGTGTTGCCAAGGT	120
<i>DXR</i> (AF182287)	GGTGATGAAGGTGTTGTTGAGGTT AGGGACCGCCAGCAATTAAGGT	160

dissociation stage at 95 °C (15 s), 60 °C (1 min), and 95 °C (15 s). Dissociation was performed to detect possible primer dimers. Each sample was performed in triplicate, and a negative control was included in all qPCR runs. Relative gene expression was calculated based on 2<sup>-ΔΔCT</sup> comparative method [30].

### Statistical analysis

All experiments were conducted at least three times, and all the values are shown as mean ± SE. Significant differences between the control and treatment groups were analyzed using one-way ANOVA procedure with SPSS 20.0 software.

## Results

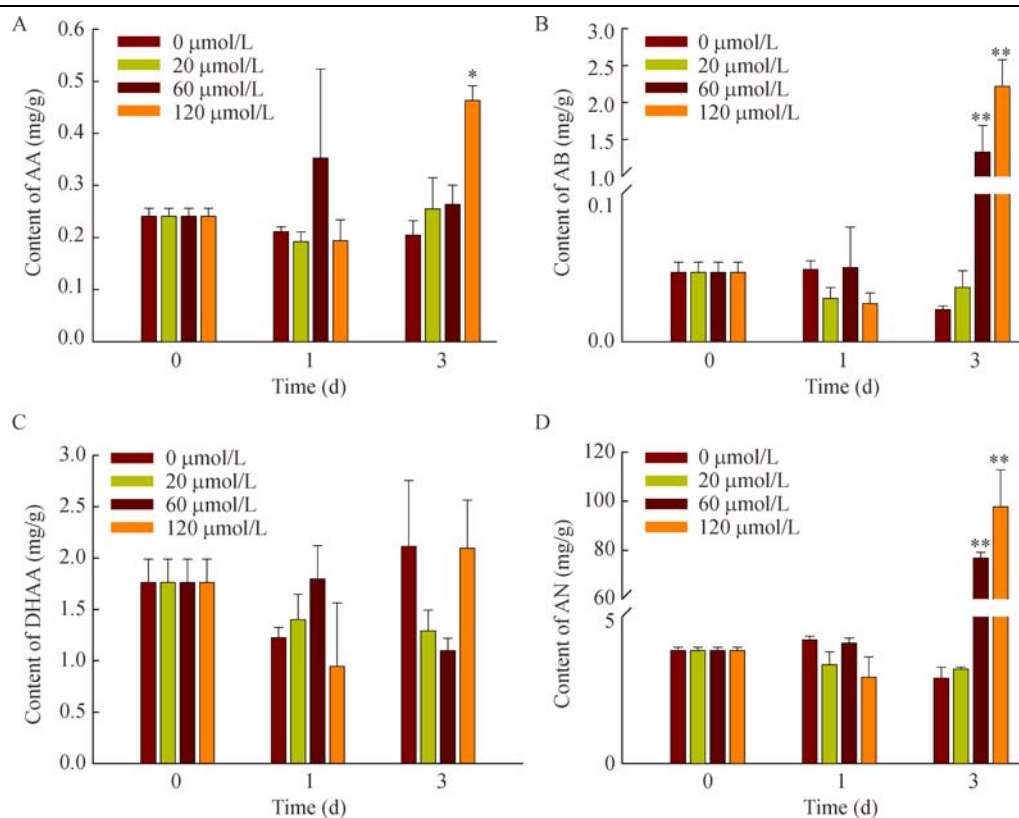
### Effects of Cd on biosynthesis of AA, AB, DHAA, and AN in *A. annua*

Fig.2 shows changes in AA, AB, DHAA, and AN concentrations after treatment with Cd at different concentrations. 1 d after treatment, the concentrations of the four metabolites showed no significant difference in all

the treated groups compared with the control group. However, after 3 d of treatment, the 60 and 120 μmol/L concentration groups showed a significant increase in AA, AB, and AN concentrations compared with the control. After 3 d of treatment with 120 μmol/L of Cd, AA, AB, and AN concentrations were 2.26 ( $P < 0.05$ ), 102.08 ( $P < 0.01$ ) and 33.63 ( $P < 0.01$ ) times that of the control. After 3 d of treatment with 60 μmol/L Cd, AB and AN concentrations were 61.10 ( $P < 0.01$ ) and 26.40 ( $P < 0.01$ ) times that of the control; the concentration of AA was slightly higher than that of the control ( $P > 0.05$ ). After 3 d of treatment with 20 μmol/L Cd, AA, AB, and AN concentrations were slightly higher than that of the control ( $P > 0.05$ ). After 3 d, the concentrations of DHAA in all treatment groups were slightly lower than that of the control ( $P > 0.05$ ).

### Effects of Cd on AN biosynthesis genes

Studies have shown that the biosynthesis and accumulation of secondary metabolites in plants are closely associated with the expression of key enzyme genes in their biosynthesis pathways [31–34]. The results above show that Cd can significantly increase the concentrations of AA, AB, and AN in *A. annua*. qPCR was used to further



**Fig. 2** Effects of different doses of Cd on AA (A), AB (B), DHAA (C), and AN (D) in *A. annua*. Vertical bars represent the standard error (SE),  $n = 3$ . Asterisks represent significant differences between treated and control *A. annua* plants at the same time (\* $P < 0.05$ , \*\* $P < 0.01$ ).

investigate the effects of different concentrations of Cd on the expression of key enzyme genes in the AN biosynthesis pathways in *A. annua*, and the relationship between the key enzyme gene expression levels and the concentrations of the four metabolites. This method was used to determine the relative expression levels of eight genes (*HMGR*, *FPS*, *ADS*, *CYP71AV1*, *DBR2*, *ALDH1*, *DXS*, and *DXR*).

Expression trends of *HMGR* and *FPS*, key enzyme genes in the upstream of AN biosynthesis pathway, were similar in the control and in all the treatment groups. Relative expression levels increased after 4 h of treatment, reaching its peak at 8 h before decreasing, and remaining consistent at 24 h, 48 h, and 72 h (Fig. 3A and 3C). Comparing the control with the treatment groups at any time point, the relative expression levels of *HMGR* and *FPS* were highest in the 120  $\mu\text{mol/L}$  group; the relative expression level of *HMGR* was 4.33 times that of the control at 8 h, and that of *FPS* was 6.95 times higher at 48 h (Fig. 3B and 3D).

*ADS* is widely acknowledged as the first key enzyme gene in the AN biosynthesis pathway. Relative expression level of *ADS* was highest at 4 h in both the control and treatment groups, then declined until reaching another peak at 48 h (Fig. 4A). The relative expression level of *ADS* was highest in the 120  $\mu\text{mol/L}$  group compared with

the control and the other treatment groups at any time point, with a relative expression level of *ADS* 112.68 times that of the control at 8 h. However, the relative expression of *ADS* was not detected at 24 h (Fig. 4B).

The expression trends of *CYP71AV1*, a multiple functional enzyme which catalyzes amorpho-4,11-diene successively into AA, were similar to that of the *ADS* in the control and in all treatment groups, with the highest level detected at 4 h, but then decreased before reaching another peak at 48 h (Fig. 4C). The relative expression of *CYP71AV1* was highest in the 120  $\mu\text{mol/L}$  group compared with that of the control and the other treatment groups at any time point, with its relative expression level 997.98 times that of the control at 48 h (Fig. 4D).

The expression trends of *DBR2*, a key enzyme specifically catalyzing artemisinic aldehyde into dihydroartemisinic aldehyde, were similar to that of *HMGR* and *FPS*, which increased at 4 h, reaching its peak at 8 h before declining, and remained constant at 24 h, 48 h, and 72 h (Fig. 5A). The relative expression level of *DBR2* was highest in the 120  $\mu\text{mol/L}$  group compared with the control and other treatment groups at any time point, with its relative expression level 62.73 times that of the control at 72 h (Fig. 5B).

*ALDH1* simultaneously catalyzes artemisinic aldehyde

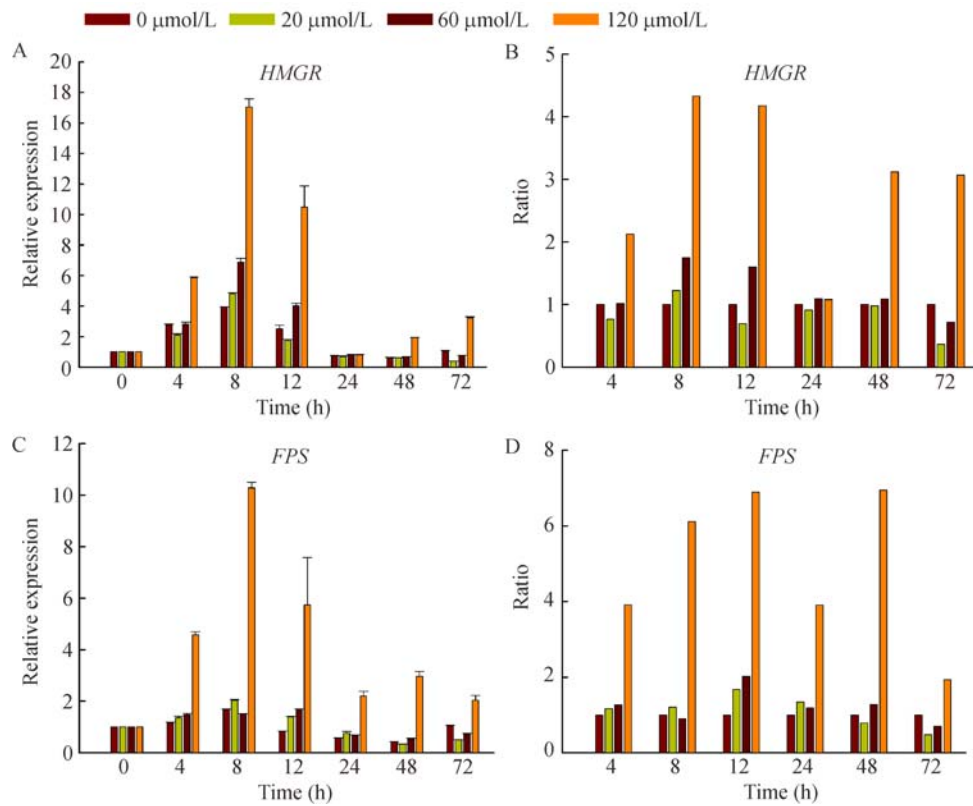


**Fig. 3** Changes in the relative expression levels (A and C) of *HMGR* and *FPS* after Cd treatment and the ratio of relative expression between treated and control *A. annua* plants at the same time (B and D). The error bars represent the standard error (SE),  $n = 3$ .

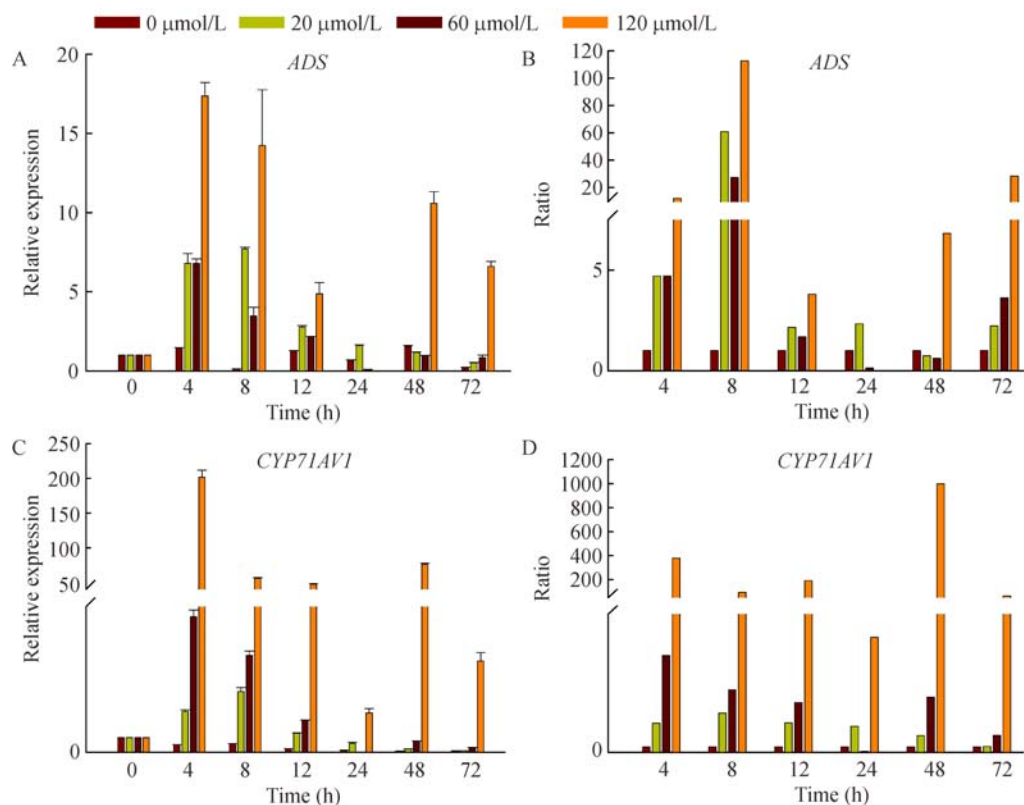


**Fig. 4** Changes in the relative expression levels of *ADS* and *CYP71AV1* (A and C) and the ratio of relative expression between treated and control *A. annua* plants at the same time (B and D) after Cd treatment. The error bars represent the standard error (SE),  $n = 3$ .



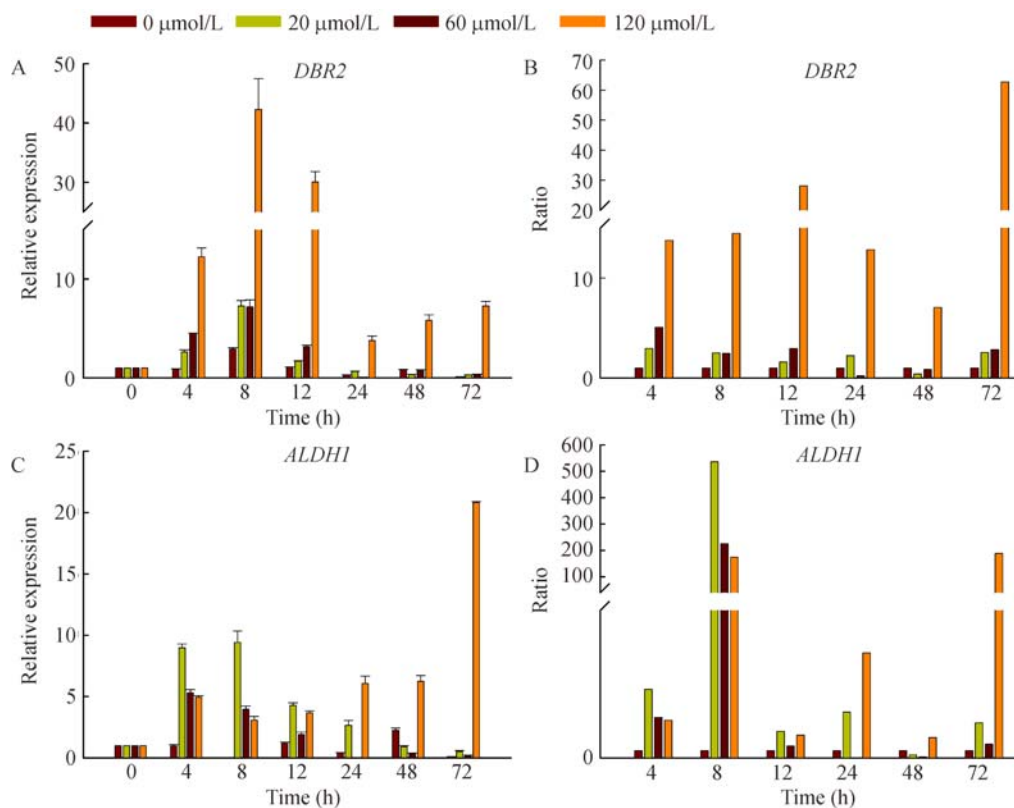


**Fig. 5** Changes in the relative expression levels (A and C) of *DBR2* and *ALDH1* and the ratio of relative expression between treated and control *A. annua* plants at the same time (B and D) after Cd treatment. The error bars represent the standard error (SE),  $n = 3$ .

into AA and dihydroartemisinic aldehyde into DHAA. The relative expression level of *ALDH1* was highest in the 20 μmol/L group compared with the control and the other treatment groups at 4 h, 8 h, and 12 h, with its relative expression level 533.76 times that of the control at 8 h. The relative expression level of *ALDH1* was highest in the 120 μmol/L group compared with the control and other treatment groups at 24 h, 48 h, and 72 h, with its relative expression level 188.70 times that of control at 72 h (Fig. 5D).

*DXS* and *DXR*, genes of key enzymes in the upstream MEP pathway, are involved in AN biosynthesis by catalyzing IPP, a precursor of AN. The expression trends of *DXS* and *DXR* were similar in the control and treatment groups, with relative expression level increasing at 4 h, reached a peak at 8 h, then decreased; remained stable at 24, 48, and 72 h (Fig. 6).

## Discussion

Changes in the concentrations of AA, AB, and AN in *A. annua* between the control and Cd-treated groups were almost the same at 1 d and 3 d after treatment. At 1 d, concentrations of all three secondary metabolites

decreased, increased, and finally decreased with increasing Cd concentration. However, at day 3, the concentrations of these metabolites increased with increasing Cd concentration. The results indicated that AA and AB showed the same trends with AN in *A. annua* after Cd treatment, but the accumulation trend of DHAA slightly differed from that of AN. Similar results were reported by Wang *et al.* [35]. To ensure that Cd influences the transcription of genes involved in artemisinin biosynthesis, we used real-time PCR for analyzing the relative expression levels of the following genes: *HMGR*, *FPS*, *ADS*, *CYP71AV1*, *DBR2*, *ALDH1*, *DXR*, and *DXS*. The relative expression levels of these eight genes reached their peak at 4 h and 8 h and then declined. In addition, the abundance of these transcripts in response to different concentrations of Cd are different during this time period. Cd might be the specific signal that causes changes in the transcript levels of *HMGR*, *FPS*, *ADS*, *CYP71AV1*, *DBR2*, *ALDH1*, and *DXR* in 120 μmol/L treatment group. However, in the 20 μmol/L and 60 μmol/L treatment groups, *ADS*, *CYP71AV1*, *ALDH1*, and *DXS* are the genes that showed changes in transcript levels.

Cd can increase the accumulation of secondary metabolites such as AN by up-regulating key enzyme genes in the AN biosynthesis pathways. The relative expression levels of *HMGR*, *FPS*, *ADS*, *CYP71AV1*,

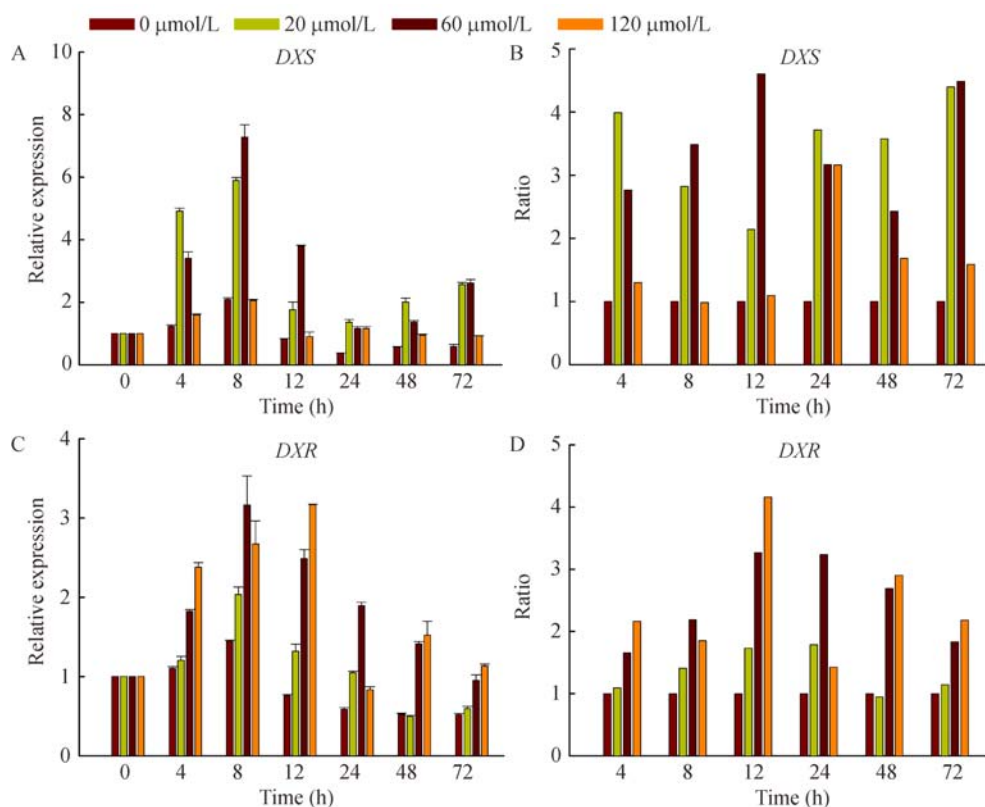


**Fig. 6** Changes in the relative expression levels (A and C) of *DXS* and *DXR* and the ratio of relative expression between the treated and control *A. annua* plants at the same time (B and D) after Cd treatment. The error bars represent the standard error (SE),  $n = 3$ .

*DBR2*, *ALDH1*, and *DXR* were highest after treatment with 120 μmol/L of Cd. These observations indicate that the concentrations of AN, AA, and AB were the highest in the group treated with 120 μmol/L Cd for 3 d; whereas the relative expression levels of *ADS*, *CYP71AV1*, *ALDH1*, and *DXS* were up-regulated in the 20 and 60 μmol/L-treated groups. These findings suggest that different concentrations of Cd showed varied effects on the expression levels of key enzyme genes in AN biosynthesis pathways, which may be the reason why concentrations of metabolites like AN differed in *A. annua* after treatment with different concentrations of Cd.

Many strains of *A. annua*, such as SP18 [14], 001 strain [16], and YU strain [15], which produce a high yield of artemisinin, and can be divided into two chemotypes, AA/AB and AN/DHAA, based on the concentrations of AA, AB, DHAA, and AN. YU and 001 strains belong to AA/AB chemotype, whereas SP18 belongs to AN/DHAA [36]. In our study, concentrations of AA, AB, DHAA, and AN in *A. annua* (guihao third) were determined by HPLC-ESI-MS/MS, and results showed that the concentrations of AN and DHAA were higher than that of AB and AA. This observation suggests that, like SP18, *A. annua* (guihao

third) also belongs to the AN/DHAA chemotype. Research has showed that AN biosynthesis pathways differed between these two chemotypes [36].

Interestingly, concentrations of DHAA in the control and treatment groups showed no significant difference. However, some studies have reported [14,31] that concentrations of DHAA significantly increased in *A. annua* (SP18) after chitosan and MeJA treatment. *A. annua* (SP18) and *A. annua* (guihao third) are both the AN/DHAA chemotype, and this difference in DHAA concentrations between these two cultivars may lie in different elicitors. DHAA, the accepted direct precursor of AN, could turn into AN and eliminate ROS simultaneously by quenching singlet oxygen in a non-enzymatic fashion [27]. This finding suggested that the presence of ROS is conducive to the transformation of DHAA to AN. Previous studies in our laboratory have shown that Cd could induce the generation of ROS in *A. annua* [10]. This result suggested that DHAA could turn into AN in *A. annua* under Cd treatment. DHAA concentration did not significantly differ between the control and treatment groups. The concentrations of AN in groups treated with 60 and 120 μmol/L Cd were significantly higher than those



in the control, suggesting that DHAA was rapidly and efficiently converted into the product AN by ROS produced after Cd treatment.

## Acknowledgements

This work was financially supported by the National Natural Science Foundation of China (Nos. 81130070, 81325023, and 81473307), Natural Key Technologies R&D Program of China (Nos. 2012BAI29B02 and 2012BAI28B02), and the Innovative Funding for PhD Students at China Academy of Chinese Medical Sciences (No. CX201608).

## Compliance with ethics guidelines

Liangyun Zhou, Guang Yang, Haifeng Sun, Jinfu Tang, Jian Yang, Yizhan Wang, Thomas Avery Garran, and Lanping Guo declare no conflict of interest. This article does not involve a research protocol requiring approval by the relevant institutional review board or ethics committee.

## References

- Dixon RA. Natural products and plant disease resistance. *Nature* 2001; 411(6839): 843–847
- Wink M. Evolution of secondary metabolites from an ecological and molecular phylogenetic perspective. *Phytochemistry* 2003; 64(1): 3–19
- Huang CY, Bazzaz FA, Vanderhoef LN. The inhibition of soybean metabolism by cadmium and lead. *Plant Physiol* 1974; 54(1): 122–124
- Larbi A, Morales F, Abadía A, Gogorcena Y, Lucena JJ, Abadía J. Effects of Cd and Pb in sugar beet plants grown in nutrient solution: induced Fe deficiency and growth inhibition. *Funct Plant Biol* 2002; 29(12): 1453–1464
- Ekmekçi Y, Tanyolaç D, Ayhan B. Effects of cadmium on antioxidant enzyme and photosynthetic activities in leaves of two maize cultivars. *J Plant Physiol* 2008; 165(6): 600–611
- Uraguchi S, Watanabe I, Yoshitomi A, Kiyono M, Kuno K. Characteristics of cadmium accumulation and tolerance in novel Cd-accumulating crops, *Avena strigosa* and *Crotalaria juncea*. *J Exp Bot* 2006; 57(12): 2955–2965
- Shi GX, Xu QS, Xie KB, Xu N, Zhang XL, Zeng XM, Zhou HW, Zhu L. Physiology and ultrastructure of *Azolla imbricata* as affected by Hg<sup>2+</sup> and Cd<sup>2+</sup> toxicity. *Acta Botanica Sinica (Zhi Wu Xue Bao)* 2003; 45: 437–444 (in Chinese)
- Vitti A, Nuzzaci M, Scopa A, Tataranni G, Remans T, Vangronsveld J, Sofio A. Auxin and cytokinin metabolism and root morphological modifications in *Arabidopsis thaliana* seedlings infected with *Cucumber mosaic virus* (CMV) or exposed to cadmium. *Int J Mol Sci* 2013; 14(4): 6889–6902
- Daud MK, Ali S, Variath MT, Zhu SJ. Differential physiological, ultramorphological and metabolic responses of cotton cultivars under cadmium stress. *Chemosphere* 2013; 93(10): 2593–2602
- Li X, Zhao M, Guo L, Huang L. Effect of cadmium on photosynthetic pigments, lipid peroxidation, antioxidants, and artemisinin in hydroponically grown *Artemisia annua*. *J Environ Sci (China)* 2012; 24(8): 1511–1518
- Zheng Z, Wu M. Cadmium treatment enhances the production of alkaloid secondary metabolites in *Catharanthus roseus*. *Plant Sci* 2004; 166(2): 507–514
- Liu D, Zhang L, Li C, Yang K, Wang Y, Sun X, Tang K. Effect of wounding on gene expression involved in artemisinin biosynthesis and artemisinin production in *Artemisia annua*. *Russ J Plant Physiol* 2010; 57(6): 882–886
- Yadav RK, Sangwan RS, Sabir F, Srivastava AK, Sangwan NS. Effect of prolonged water stress on specialized secondary metabolites, peltate glandular trichomes, and pathway gene expression in *Artemisia annua* L. *Plant Physiol Biochem* 2014; 74: 70–83
- Lei CY, Ma DM, Pu GB, Qi XF, Du ZG, Wang H, Li GF, Ye HC, Liu BY. Foliar application of chitosan activates artemisinin biosynthesis in *Artemisia annua* L. *Ind Crops Prod* 2011; 33(1): 176–182
- Arsenault PR, Vail DR, Wobbe KK, Weathers PJ. Effect of sugars on artemisinin production in *Artemisia annua* L.: transcription and metabolite measurements. *Molecules* 2010; 15(4): 2302–2318
- Pu GB, Ma DM, Chen JL, Ma LQ, Wang H, Li GF, Ye HC, Liu BY. Salicylic acid activates artemisinin biosynthesis in *Artemisia annua* L. *Plant Cell Rep* 2009; 28(7): 1127–1135
- Caretto S, Quarta A, Durante M, Nisi R, De Paolis A, Blando F, Mita G. Methyl jasmonate and miconazole differently affect artemisinin production and gene expression in *Artemisia annua* suspension cultures. *Plant Biol (Stuttg)* 2011; 13(1): 51–58
- Duke SO, Paul RN. Development and fine structure of the glandular trichomes of *Artemisia annua* L. *Int J Plant Sci* 1993; 154(1): 107–118
- Akhila A, Thakur RS, Popli SP. Biosynthesis of artemisinin in *Artemisia annua*. *Phytochemistry* 1987; 26(7): 1927–1930
- Towler MJ, Weathers PJ. Evidence of artemisinin production from IPP stemming from both the mevalonate and the nonmevalonate pathways. *Plant Cell Rep* 2007; 26(12): 2129–2136
- Bouwmeester HJ, Wallaart TE, Janssen MH, van Loo B, Jansen BJ, Posthumus MA, Schmidt CO, De Kraker JW, König WA, Franssen MC. Amorpho-4,11-diene synthase catalyses the first probable step in artemisinin biosynthesis. *Phytochemistry* 1999; 52(5): 843–854
- Ro DK, Paradise EM, Ouellet M, Fisher KJ, Newman KL, Ndungu JM, Ho KA, Eachus RA, Ham TS, Kirby J, Chang MC, Withers ST, Shiba Y, Sarpong R, Keasling JD. Production of the antimalarial drug precursor artemisinic acid in engineered yeast. *Nature* 2006; 440(7086): 940–943
- Teoh KH, Polichuk DR, Reed DW, Nowak G, Covello PS. *Artemisia annua* L. (Asteraceae) trichome-specific cDNAs reveal CYP71AV1, a cytochrome P450 with a key role in the biosynthesis of the antimalarial sesquiterpene lactone artemisinin. *FEBS Lett* 2006; 580(5): 1411–1416
- Zhang Y, Teoh KH, Reed DW, Maes L, Goossens A, Olson DJ, Ross AR, Covello PS. The molecular cloning of artemisinic aldehyde  $\Delta 11(13)$  reductase and its role in glandular trichome-dependent biosynthesis of artemisinin in *Artemisia annua*. *J Biol*

- Chem 2008; 283(31): 21501–21508
25. Teoh KH, Polichuk DR, Reed DW, Covello PS. Molecular cloning of an aldehyde dehydrogenase implicated in artemisinin biosynthesis in *Artemisia annua*. *Botany* 2009; 87(6): 635–642
  26. Wallaart TE, Bouwmeester HJ, Hille J, Poppinga L, Maijers NC. Amorpho-4,11-diene synthase: cloning and functional expression of a key enzyme in the biosynthetic pathway of the novel antimalarial drug artemisinin. *Planta* 2001; 212(3): 460–465
  27. Wallaart TE, Lubberink HG, Woerdenbag HJ, Pras N, Quax WJ, Quax WJ. Isolation and identification of dihydroartemisinic acid from *Artemisia annua* and its possible role in the biosynthesis of artemisinin. *J Nat Prod* 1999; 62(3): 430–433
  28. Han XL, Huang LQ, Guo LP, Li MJ, Liu XH, Zhang XB. Accumulation and translocation of cadmium in soil and plant and its effects on growth of *Artemisia annua* and artemisinin content. *China J Chin Materia Medica (Zhongguo Zhong Yao Za Zhi)* 2010; 35(13): 1655–1659 (in Chinese)
  29. Jessing KK, Juhler RK, Strobel BW. Monitoring of artemisinin, dihydroartemisinin, and artemether in environmental matrices using high-performance liquid chromatography-tandem mass spectrometry (LC-MS/MS). *J Agric Food Chem* 2011; 59(21): 11735–11743
  30. Schmittgen TD, Livak KJ. Analyzing real-time PCR data by the comparative C(T) method. *Nat Protoc* 2008; 3(6): 1101–1108
  31. Cheng Q, Su P, Hu Y, He Y, Gao W, Huang L. RNA interference-mediated repression of SmCPS (copalylidiphosphate synthase) expression in hairy roots of *Salvia miltiorrhiza* causes a decrease of tanshinones and sheds light on the functional role of SmCPS. *Biotechnol Lett* 2014; 36(2): 363–369
  32. Gu XC, Chen JF, Xiao Y, Di P, Xuan HJ, Zhou X, Zhang L, Chen WS. Overexpression of allene oxide cyclase promoted tanshinone/phenolic acid production in *Salvia miltiorrhiza*. *Plant Cell Rep* 2012; 31(12): 2247–2259
  33. Shen Q, Chen YF, Wang T, Wu SY, Lu X, Zhang L, Zhang FY, Jiang WM, Wang GF, Tang KX. Overexpression of the cytochrome P450 monooxygenase (cyp71av1) and cytochrome P450 reductase (cpr) genes increased artemisinin content in *Artemisia annua* (Asteraceae). *Genet Mol Res* 2012; 11(3): 3298–3309
  34. Xiang L, Zeng LX, Yuan Y, Chen M, Wang F, Liu XQ, Zeng LJ, Lan XZ, Liao ZH. Enhancement of artemisinin biosynthesis by overexpressing dxr, cyp71av1 and cpr in the plants of *Artemisia annua* L. *Plant Omics* 2012; 5: 503–507
  35. Wang HH, Ma CF, Li ZQ, Ma LQ, Wang H, Ye HC, Xu GW, Liu BY. Effects of exogenous methyl jasmonate on artemisinin biosynthesis and secondary metabolites in *Artemisia annua* L. *Ind Crops Prod* 2010; 31(2): 214–218
  36. Wang H, Ma C, Ma L, Du Z, Wang H, Ye H, Li G, Liu B, Xu G. Secondary metabolic profiling and artemisinin biosynthesis of two genotypes of *Artemisia annua*. *Planta Med* 2009; 75(15): 1625–1633